J. Comput. Appl. Res. Mech. Eng. Vol. 11. No. 1, pp. 243-255, 2021 *DOI: 10.22061/JCARME.2020.5977.1763*

Journal of Computational and Applied Research in Mechanical Engineering

jcarme.sru.ac.ir

SRTTU

JCARME

ISSN: 2228-7922

Research paper

Solid-phase effects on the performance of a centrifugal slurry pump using computational fluid dynamics

Mohammad Reza Aligoodarz*, Mohsen Dalvandi and Abdollah Mehrpanahi

Department of Mechanical Engineering, Shahid Rajaee Teacher Training University, Tehran, Iran

Article info:

Article history:

Received: 17/09/2019

Revised: 13/05/2020

Accepted: 15/05/2020

Online: 17/05/2020

Keywords:

Centrifugal slurry pump,

Numerical simulation,

Slurry flow,

CFX,

Turbulence.

***Corresponding author:**
maligoodarz@sru.a.cir

Abstract

The centrifugal slurry pump is the most common slurry flow pump used in mining industries. The pump head and efficiency are affected by the size, concentration, and density of solid particle when these pumps are applied for the control of slurries. Because the suspended solids in the liquid could not well absorb, store, and transmit pressure energy, they cause quite different changes in efficiency and performance curve shape. This study was conducted to investigate the variations of the mentioned factors at different flow rates using a numerical simulation of the centrifugal slurry pump. For this purpose, the 3D turbulent flow was solved by applying Reynolds-Averaged Navier-Stokes (RANS) equations using the Shear Stress Transfer (SST) turbulence model based on Eulerian-Eulerian for 45% to 120% flow rates in CFX (Ver. 17) software. The accuracy of the numerical solution was investigated by comparing the characteristic curves resulting from the numerical solution with experimental data. The obtained results show a satisfactory fitting among the calculated values from the numerical analysis and experimental data to predict pressure and velocity distribution and global performance. Moreover, by simulating the effect of different parameters of the slurry flow, their effect on the characteristic curves of the slurry pump was compared. These results reveal that the numerical solution can efficiently predict the variation trend of the slurry flow parameters.

1. Introduction

A mixture or combination of any liquids with solid particles is named slurry or two phases flow of solid-liquid [1]. Various types of pumps are used in slurry ones. Centrifugal slurry pump is one of the common and essential equipment in the mineral industry. The basis of its operation is based on the transfer of angular momentum from the wheel to the flowing fluid. Differences of slurry properties such as volumetric concentration, particle size, and density cause pump performance decline. Due to the dispersion, two-phase flow physics is more complicated than singular-phase; its complexities arise when the flow is turbulent by oscillation or continuous collision of particles, thus solid phase interact directly with liquid phase components. Particle movement of two-phase flow causes flow disturbance and affects

speed field and flow pressure. Also, the proper knowledge of transport of mixtures is needed for the design of transmission systems. In the previous experimental studies, input parameters and flow properties variation were considered to extract output diagrams like head-flow, wear rate, efficiency-flow, pressure drop, and power-flow. In the case of head-flow, Yajima et al. [2] presented the water-head slurry ratio diagram reduced with increasing the volumetric concentration and relative particle size, but this trend showed a non-linear behavior. Gandhi et al. [3] assessed the functional attributes of the centrifugal slurry pumps at various speeds of water and solid-liquid mixture. They found that the common equation of flow-head can be applied to slurry pumps in low concentrations (weighing concentration less than 20%). In higher concentrations, these equations must be changed with respect to solids.

Another research line in this field is wear rate assessment investigated by Pagalthivarthi et al. [4-5]. They carried out two studies on the wear rate at the slurry pump, somehow, they simulate slurry flow in the two-dimensional cochlear model. Variable parameters conclude volumetric concentration and particle size whose increase causes the growth of wear rate. Indeed, several changes in experimental designs were performed in order to improve the wear rate. Results show that the reduction of the distance between the scallops and increase of scroll width lead to the decline of wear rate. The efficiency and related parameters in the slurry pumps have been investigated in various studies. In this field, Mehta et al. obtained slurry particle velocity in a centrifugal slurry pump with using speedometer technique and the adaptive refractive index of light. Experiments on the slurry pump were carried out by prepared slurry gained from sodium iodide as an effective fluid and glass beads with a mean diameter of 500µm with the volumetric concentration of 1, 2 and 3% at speed of 725 and 1000 rpm. The highest velocities in the impeller blade occur on the blade suction side and edge of the entrance blade. The mean particles velocity and their kinetic energy drop with an increase of concentration, on the other hand, the maximum kinetic energy exists at the blade suction side [6].

Wennberg and his colleagues discussed various experiments of slurry pumps and the maximum permitted reduction of head and efficiency respectively are 10 and 15 regarding keep constant head amount. The increase of shock loss, vortex flow and slurry blockage in the pump inlet area have been assessed as a mechanism for supporting the unstable head curve [7]. Pressure drop is the main subject for extracting an acceptable system performance. In this filed and using the validated data, Kumar et al. simulate numerically based on field data to calculate the pressure drop during a 90° bend of a silicon-bearing tube. Three different volumetric concentrations (3.94, 8, 8.2%) with a particle size of 448.5µm at speeds of 1.78 to 3.56% were defined. The pressure in the outer wall was larger than the inner wall; and also speed distribution and solid particles concentration were more uniform in the downstream flow. Velocity, pressure and concentration profile are not affected by tube bending [8]. The efficiency could be affected by the practical flow situation. Huang et al. simulated a solid-liquid phase flow of centrifugal pump using a discrete element method by fluent software. In this study, the flow in a one-stage was analyzed transiently regarding the interaction of particle-particle and particle-wall. Water under the condition of 25°C as a continuous phase with 15% volume, its density 1500 kg/m3 with a particle diameter of 1 to 3mm, was simulated. Results showed the influence of particle movement on the flow performance during a time in the center of the centrifugal pump, also velocity field for two-phases and particle movement route was demonstrated [9].

The most important method of fluid flow analysis is the use of CFD-based analysis [10-12]. Advancements in computer and software technology particularly fluid dynamics lead to the novel methods of the two phases flow equation in centrifugal pumps; the interface between two phases is influenced by relative movement phases. Generally, two distinct methods exist. Using the Navier-Stokes equations play a crucial role in CFD analysis [13-14].

The Navier-Stokes equations are used to calculate the initial phase of flow in which a number of particles represent the total particle flow. The force equilibrium equation is solved according to the second law of Newton to calculate the discrete phase path. If the fraction of the dispersed phase volume is small, it would

be appropriate and would provide complete information of its function and time of particle deposition. The Eulerian-Eulerian approach is the most common approach to multiphase flow, in that each phase is controlled by the Navier-Stokes equation. Each phase is characterized by its physical properties and its velocity, pressure, and temperature. The Eulerian-Eulerian approach can be applied in dispersed-continuous and continuous-continuous systems. In the dispersed-continuous system, the velocity of each phase is calculated using the Navier-Stokes equations, effective forces are modeled empirically and are referred to as a section of the fuzzy transfer. Moreover, the effects of the gravity, flotation, and virtual mass are seen in dispersed phase [15].

In the recent study, which is performed by Shi and Wei, the Numeral simulation of 3D turbulent flow in a low specific speed solid-liquid centrifugal pump has been considered. In this research the 3D turbulent flow fields in pumps have been simulated for the ash-particles with the volume fraction of 10 t0 30% at a similar particle diameter. In addition, the two-phase calculation results are compared with those of single-phase clean water flow. The results showed that the strategy is greatly helpful to the solution convergence. Moreover, the results gave the main area of the abrasion of the impeller and volute casing and improve the design of the impeller in order to increase the service life of the pump [16].

In this paper, two phases of slurry flow in the 4.9-inch slurry pump of Warman were evaluated. Researchers include the definition of the centrifugal pump geometry, the production, and independence of the network. Discretization of equations of fluid flow requires finite volume method in CFX code; also, the turbulence model is Shear-Stress-Transport (SST) proposed by Menter [17].

Due to the importance of these types of pumps, several kinds of research have been published recently [18-20]. In this paper, after validation of numerical analysis with using the experimental data of references, important parameters like velocity, volume, concentration, particle size, and particle density have been considered; also, the effects of these parameters on efficiency are evaluated. The amount of head and efficiency was considered for slurry and water, the head loss values for every parameter were determined as well as regarding equal parameters of concentration; particle size and particle density for slurry flow at three various rotary velocities were considered. For identification of particle accumulation in the pump, volumetric particle contours were shown at three volumetric concentrations.

2. System introduction

Variable parameters include concentration, particle size, a density of slurry pump, specific weigh of solid particles and particle distribution which are measurable. The average diameter of particles is also obtained from Eq. (1).

$$d_w = \sum_{i=1}^{n} x_i d_i \tag{1}$$

n is the number of aggregates in which all particles are classified, x_i is equal to the weight fraction of solid particles remaining on the sieve with the specified degree. $d_i = 30.13 \mu m$ is the average of the arithmetic of two sequential aggregates. Considering the water density (ρ_l) as well as the water specific weigh (ρ_s), at various concentrations (C_w), the density of slurry flow is obtained as follows:

$$\rho_m = \frac{100}{\left(C_w / \rho_s\right) + \left((100 - C_w) / \rho_l\right)} \tag{2}$$

The volume concentration (C_v) is obtained using Eq. (3): [1]

$$C_V = \frac{C_w}{\rho_s (1 - C_w) + C_w} \tag{3}$$

Table 1 shows slurry densities and volumetric concentrations for different weight concentrations:

Table 1. Slurry density and volumetric concentration for concentrations different weight.

No	Volumetric concentration (%)	Slurry density (kg/m^3)	Weigh concentration (%)
1	11	1180	25
2	16.8	1270	35

3	23	1380	45

2.1. Geometric properties of the centrifugal slurry pump

An industrial single stage and suction pump from Warman Corporation have been selected as the model used for simulation. Geometric parameters with its performance characteristics are summarized in Table 2. The material of components pump is cast iron. Also with Solidworks software, the pump was modeled. Its constituents are shown in Fig. 1.

3. Numerical modeling

Two phases slurry are made of two distinct solid-liquid phases separated by common surfaces and dynamically have interacted at these levels. In liquid-solid dual-phases flows, the fluid phase (as the carrier phase) is completely continuous and the solid phase (as the particle phase or dispersed phase) is in the form of separate particles. In order to calculate the flow of the pump, the equations of mass survival, momentum, and transmission equation for turbulent two-phase flow parameters were used also for consideration of two phases interaction, Euler-Euler was applied. Regarding mathematical equations, various phases flow are evaluated as continuous interacting environments. Since the volume of a phase cannot be occupied by another phase, the concept of the fuzzy volume fraction is introduced as equations. The volume fraction of phases are defined by space and position and their sum is equal to1 [8]. Momentum equation and continuity were solved for each phase by the Ulrich model. The relation between these equations is carried out through pressure and fuzzy exchange coefficients. A multiple coordinate system is used to account the effect of the pump wheel rotation. The continuity and momentum equations for an incompressible two-phase flow are written in 4-7 with the assumption of constant state [21]:

$$\left(\frac{\partial(\rho_l \alpha_l)}{\partial t} + \nabla\left(\rho_l \alpha_l \overline{V}_l\right)\right) = 0 \tag{4}$$

$$\left(\frac{\partial(\rho_s \alpha_s)}{\partial t} + \nabla\left(\rho_s \alpha_s \overline{V}_s\right)\right) = 0 \tag{5}$$

$$\rho_l \alpha_l \left(\frac{\partial \overline{V}_l}{\partial t} + \overline{V}_l.\nabla \overline{V}_l\right) = -\alpha_l \nabla \mathrm{P} + \nabla.\alpha_l \overline{\overline{\tau}}_l + \alpha_l \rho_l \overline{\mathrm{g}} - \beta(\overline{V}_l - \overline{V}_s) \tag{6}$$

$$\rho_s \alpha_s \left(\frac{\partial \overline{V}_s}{\partial t} + \overline{V}_s.\nabla \overline{V}_s\right) = -\alpha_s \nabla \mathrm{P} + \nabla.\overline{\overline{\tau}}_s - \nabla \mathrm{P}_s + \alpha_s \rho_s \overline{\mathrm{g}} + \beta(\overline{V}_l - \overline{V}_s) \tag{7}$$

where I and S are descriptive of solid and liquid phase respectively, α represents fuzzy volumetric fraction, and V is phase velocity. Massive force and virtual mass are negligible in the momentum equation. Stress tensor of each phase in the equations is accordance to Eq. (8) [22].

$$\overline{\overline{\tau}}_q = \alpha_q \mu_q \left(\nabla \overline{V}_q + \nabla \overline{V}_q^T\right) + \alpha_q \left(\lambda_q - \frac{2}{3}\alpha_l \overline{V}_l \mu_q\right) \nabla \overline{V}_q \overline{\overline{I}} \tag{8}$$

Table 2. The geometry and design of the Warman 6/4 pump used [22].

Parameters	Quantity
The diameter of the exit pump impeller	371mm
The width of the exit pump impeller	51mm
Impeller type	Close
Number of blades	6
Blade input angle	20°
Blade output angle	23°
Diameter of inlet suction	150mm
Overlapping angle of blades	125°
Clearance between impeller and screw section of pump	38mm
The angle of screw tab	72°

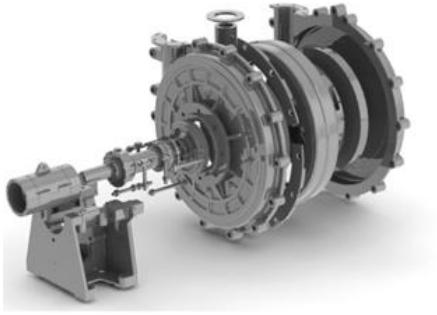

Fig. 1. The 3D geometry model of the centrifugal slurry pump.

where μ and λ are shear viscosity and phase mass viscosity, respectively. The fuzzy exchange coefficient (β) presented in Eq. (6) and Eq. (7) is given by Gidaspow et al. which contain the expressions provided by Wen–Yu [21].

$$\forall \alpha_l > 0.8 \Rightarrow$$

$$\beta = \frac{3}{4} C_D \frac{\alpha_s \alpha_l \rho_l \left| \overline{V_s} - \overline{V_l} \right|}{d_s} \alpha_l^{-2.65} \quad (9.a)$$

$$\forall \alpha_l \leq 0.8 \Rightarrow$$

$$\beta = 150 C_D \frac{\alpha_s (1-\alpha_l) \mu_l}{\alpha_l d_s^2} + 1.75 \frac{\rho_s \alpha_s \left| \overline{V_s} - \overline{V_l} \right|}{d_s} \quad (9.b)$$

According to Eqs. ((9. (a and b)) also the coefficient drag (C_D) of Eq. (10) is defined based on Reynolds number of particles in Eq. (11) [21].

$$C_D = \frac{24}{\alpha_s Re_s} \left[1 + 0.15 (\alpha_l Re_s)^{0.687} \right] \quad (10)$$

$$Re_s = \frac{\rho_l d_s \left| \overline{V_s} - \overline{V_l} \right|}{\mu_l} \quad (11)$$

3.1. Numerical analysis

In this paper dual-phase slurry, static, three dimensional, incompressible and confluent flows inside a centrifugal slurry pump have been simulated in CFX and Finite Element Method (FEM) has been used to solve the transport equations. Shear stress transfer (SST) was chosen to model the turbulent in which the advantages of the current away from the k-ε wall were combined with the near-wall flow k-ε; also SST model was applied in the prediction of flow separation. It is proposed as an appropriate option for simulation of turbomachinery. Automatic wall function was used on walls with respect to the value of y in the first cell on the solid surface from the lower Reynolds to the wall-logic function was changed [23]. The multiple coordinate methods were used to simulate the static and rotating components simultaneously. In order to connect fixed and rotating parts, the interface of fixed rotary was used by which the detection of local variation in wheel outflows and the interaction of fixed and mobile components has the relative superiority compared to other methods. Fixed pressure boundary conditions at entry with constant mass flow and discharge with non-slip condition in the solid-walls have been applied [24]. In the permanent state of the pump, the condition of the wheel blades and the screw cone play the crucial role in determining the flow field inside the pump, position and the area of separation [25]. With regards to roughness increase, friction and thickness of the boundary layer, the roughness of all walls in the pump should be determined in modeling pump. The roughness in the software CFX is defined by the roughness of the sand grains equivalent to the measured roughness [26]. The slurry Warman pump is made of cast iron and its surface has not been plastered; then its roughness has been calculated in a laboratory. There are also equations for estimation roughness of sand grains based on the roughness measured in the work of Adams and his colleagues; the equivalent value of sand grains for cast iron is 260μm which was applied in this paper. The convergence criterion is 10-5 [27]. To complete the repeat process in numerical computation, two control criteria have been used. The reduction of the residual error of each equation is less than 10-5 and the stability of the amount of pump outlet pressure has been considered in more than 50 last replicates in each of solving steps [28]. In examing the pump with the assumption of constant state, the flow field is determined for a given state, with regards to the position of the fixed and rotary components relative to each other [29]. It is also essential that input and output boundaries go upstream and downstream to some extent. Adding input and exit pipes to the model near the boundaries the occurrence of eddy areas will be prevented that will cause the stability of numerical analysis and better convergence of simulation.

The CFX code uses the coupler solver; in this method all simultaneous equations are solved in a vector form on each cell. In this approach, the non-explicit method for equations in every step of time is used. In a stable solution, the time step is similar to an accelerator parameter to drive approximate solutions in a physical state to

constant solutions which reduce the number of repetitions needed for convergence of the permanent solutions [24]. The pressure and velocity variables (velocity components) are simultaneously determined by the equation solving system. The solution method is implicit for equations and are solved till getting to the stable state at any time [30].

3.2. Computational domain networking

As shown in Fig. 2, computational domain consists of a propeller spiral compartment including incoming and outcoming area. Gridding was performed by Ansys Mesh Software.

Discretization of the domain of solution was carried out through a combination of networks with the organization and non-organizations. The pump wheel and the input and output components are discontinued by the hexagonal elements and the spiral compartment by four elements. Gridding is performed so that the computational elements which are close to the walls are smaller, leading to the value of y. on the wall that is smaller than 30. The effect of the size of the element is performed by the independence test of the network to ensure the numerical solution. Like previous research, simulation for several networks is repeated with the various number elements [31].

The head values according to Eq. (12) are obtained from the total differential pressure at the inlet and outlet, which is expressed by driving by the specific gravity of the fluid in the meter.

$$H = \frac{\left(P_{tot}\right)_{outlet} - \left(P_{tot}\right)_{inlet}}{\rho g} \tag{12}$$

Because of the limitation of the numerical model in the calculation of some losses such as mechanical losses in bearing, leakage losses and immortality, having the total efficiency is difficult so losses should be replaced by semi-experimental relations [32]. Ghaderi and his colleagues [33] succeeded in calculating the total efficiency as a function of other casualties, in the form of Eq. (13).

$$\eta = \left(\frac{1}{\eta_h \eta_v} + \frac{\Delta P_d}{\rho g Q H} + 0.03 \right)^{-1} \tag{13}$$

ΔP_d is disc mortality, η_v is volumetric efficiency and 0.03 is added because of the effect of losses bearing and seals. Details of this calculation were seen in Eqs. (14a, b, 15, and 16) [31].

$$\forall N_S > 65 \Rightarrow \quad \Delta P_d = 1.1 \times 75 \times 10^{-6} \rho g u_2^{\,3} D_2^{\,2} \tag{14.a}$$

$$\forall N_S < 65 \Rightarrow \quad \Delta P_d = 0.133 \times 10^{-3} \rho \times \left[2.5 \times 10^5 \omega D_2^{\,2} \right]^{0.134} \omega^3 \frac{D_2^{\,5}}{8} \tag{14.b}$$

$$N_s = \frac{3.65 N\,(rpm) \sqrt{Q\left(m^3/s\right)}}{H^{0.75}(m)} \tag{15}$$

$$\eta_v = \frac{1}{1 + 0.68 N_s^{(-0.67)}} \tag{16}$$

4. Results and discussion

The results will be presented in two sections of the results including mesh gridding and the results of fluid flow modeling at the considered conditions.

4.1. Mesh grid results

The goal of the grid theory independent solution is to bring the results convergence with a constant value.

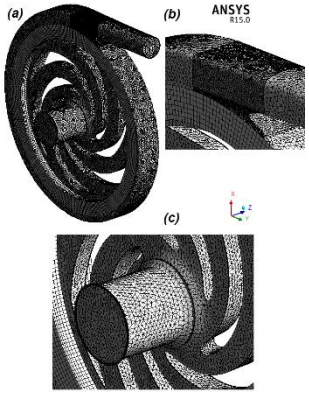

Fig. 2. The view of (a) general areas with (b) unstructured and (c) structured grids.

In the new condition, the grid will be modified sequentially, the elements number will increase and this leads to smaller units. To validate numerical results, sensitivity analysis of network is important. The effect of the size of the element is performed by the independence test from the network to ensure a numerical solution. So, simulation is repeated for several networks with the number of different elements. The result of the independence test is shown in Fig. 3. By increasing the number of elements excessive of the limit in the diagram, the calculated head value does not change significantly. In Table 3, the final results of the value of network elements in the pump components are shown.

4.2. Numerical modeling results

In this section, the results of modeling are presented in four sections. This categorization, as previously stated, is based on the importance of effective parameters on the system performance.

4.2.1. Head-discharge variations based on particle concentration

Burgess and et al. [22] provided complete information about head-power and the efficiency of water pumping and two-phase mixture in experiments, there is a good agreement between the numerical result and experimental data in the range of the nominal discharge. Also, the maximum calculated relative error is less than 6%; it indicates the good numerical accuracy of the testing model. In addition, details of uncertainties and experimental errors can be found in reference [20] which is related to control, the measure of slurry concentration, measurement error, and calculation error of pressure and density. Therefore repeatability plays an important role in results.

The head-discharge curves of numerical solution and experimental data are shown in Figs. 4, 5, and 6. These graphs were extracted for particles with $d_s = 250\mu m$ at the volumetric concentration of (25, 35 and 45%) and a specific density ($\rho_s = 2650\, kg/m^3$). In the Fig. 4 with increasing discharge at constant weight concentration of solid phase, the head value was decreased. In Fig. 5 taking into account of weighting concentration of 35%, the amount of head will decrease more than the concentration of 25% that this reduction head in Fig. 6 where the concentration (45%) is greater. As can be seen in Figs 5-7, with the increase of concentration by weight, the pump head has not changed significantly. In the field of fluid behavior, linear behavior is obtained from all three experimental cases. In contrast, due to the complexity of the solutions and the considerable uncertainties, the non-linear pump behavior has obtained and the pump behavior cannot be predicted, accurately.

Table 3. The final number of element of the pump components.

No	Components of pump	Element numbers
1	Entrance tube	126305
2	Impeller section	945446
3	Screw section	992556
4	Exit tube	162345

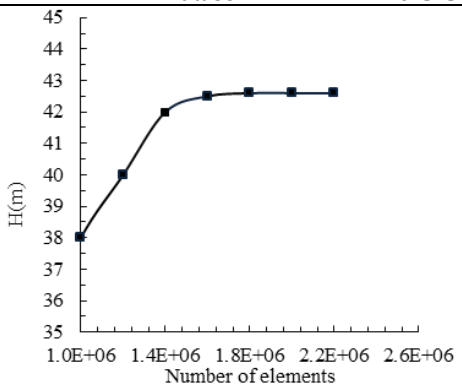

Fig. 3. The mesh independency examination.

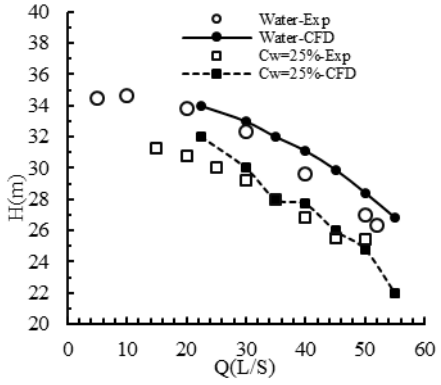

Fig. 4. Numerical and experimental [22] results of Head for water and slurry at 1200 rpm in concentration by weight 25%.

4.2.2. Efficiency-discharge diagram based on particle concentration

The total discharge-efficiency diagram for the numerical results was shown in Fig. 7. This diagram has been extracted for particles with a similar aforementioned physical condition. With keeping of pump speed in slurry flow and growth of discharge, efficiency is heightened proportionally; and in the estimated conditions it reaches its maximum limit at the best working point for all three weight concentrations; after that by enhancement of discharge value to estimated condition it gets reduced. As shown in Fig. 7, for particles with $d_s = 250\mu m$, efficiency degrades with the rising concentration of slurry flow in all discharge values. The turbulence of two-phase current flow causes the dispersed phase undergoe oscillation or continuous collision of particles; in this situation, the solid phase does not follow the flow but it is reactivated with the fluid phase components and corrected with them. Particle movements in a mixture of two-phase flows influence the structure of the turbulent phase of the fluid phase or the liquid phase and flow equilibrium.

The characteristic curve of the head-discharge for the numerical results for different diameters of particles of 10 to 300µm is shown in Fig. 8. This diagram is depicted for the best discharge point at a concentration of 25% and a speed of 1200rpm and supposed density of particles in the previous analysis. This figure shows that the pump head does not change much when the particle diameter is less than 200µm. Maximum head drop in performance curve is in particles with diameter of d_s=300µm since the required energy to float particles increases with increasing diameter, as a consequence the hydraulic performance of centrifugal slurry pump drops in order to prevent head reduction and maintenance of high efficiency in two phases of pump; particle size must be less than 50µm.

The characteristic curve of the head-discharge of numerical results for different densities of particles is shown in Fig. 9. This diagram is depicted for the best point at a weight concentration (25), the rotational speed of 1200rpm and a specific particle diameter (250µm). In this figure, little changes were observed with increasing density. It should be noted that, when the particle density is considered less than $2650\,kg/m^3$, the head changes are not very clear.

From Figs. 8 and 9 and concentration graphs, it can be found that the effects of particle density on the hydraulic performance of the pump are not as apparent as the two parameters of concentration and particle diameter.

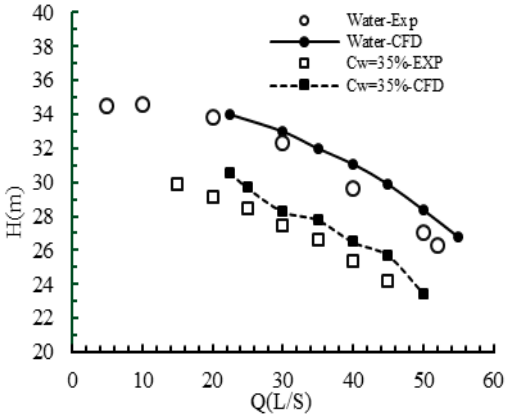

Fig. 5. Numerical and experimental [22] results of head for water and slurry at 1200 rpm in concentration by weight 35%.

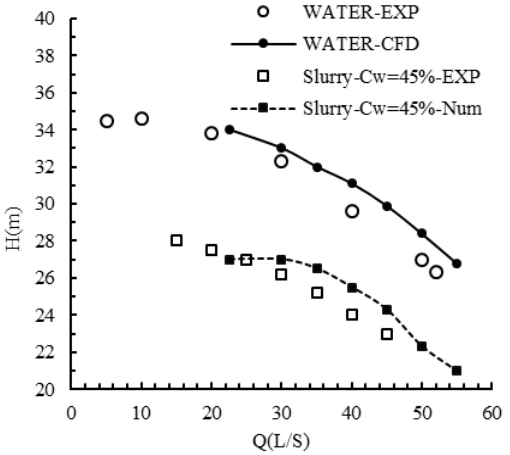

Fig. 6. Numerical and experimental [22] results of head for water and slurry at 1200 rpm in concentration by weight 45%.

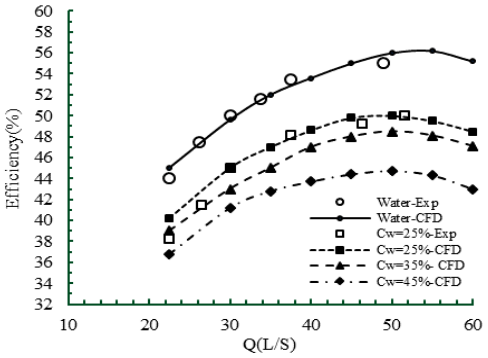

Fig. 7 Numerical and experimental [22] results of efficiency for water and slurry at 1200 rpm in concentration by weight 25%, 35% and 45%.

4.2.3. Pressure contour in slurry flow

The total pressure contours of the slurry pump at concentrations of 25, 35 and 45% in the nominal discharge and the rotational speed of 1200rpm are shown in Fig. 10. According to Fig. 10 in the fluid inlet, maximum pressure occurs at impeller section that gradually increases with closing to its edge, but in the back of the blade, it is almost negative, putting in suction mode and the value of pressure is greater at higher concentration. The pressure in the spiral section of pump move toward spiral's path gradually increases due to the approximate growth of cross-section area and the conversion of dynamic pressure to static pressure. Having constant cross-section, its pressure does not change noticeably, also input and output pressure difference decreases with increasing concentration, this pressure reduction ultimately is defined as a reduction of the pump head. Tables 4 and 5 show the variations of drop percentage of slurry pump head depending on the concentration at the different rotational speed.

As shown in Table 4, more concentration of slurry flow leads to more drop head. In addition, at a constant concentration of slurry flow, increscent rotation makes the reduction of the slurry pump head. Regarding Table 5, increasing of slurry flow concentration causes the efficiency to be heightened also at higher concentration, the drop of head and efficiency is more significant. Also at the low rotation, concentration incensement results to reduction of efficiency rate compared to head.

Table 6 shows the slurry pump head amount based on particle diameter at different rotary velocities and aforementioned particle density. Table 7 shows the slurry pump head variation percentage based on the rotational speed at a considered constant diameter (250μm).

As shown in Table 6, the slope of the head changes in particles with the diameter of 200μm and smaller of it, is lower than larger particle up to 250 μm diameters. As can be seen in this table, with the increase in pump speed and particle diameter, the pump head will decrease and increase, respectively. Due to the intended values for the pump rotation, the effect of particle size had a much greater effect on the head drop value.

In Table 7, head drop values along with increasing particle density at various rotational speeds are observed. Similar to Table 6, in this table, with the increase in pump speed and particle density, the pump head will decrease and increase, respectively. Due to the intended values for the pump rotation, the effect of particle density had a much greater effect on the head drop value. Regarding numerical analysis and simulation, it can be concluded that among variable parameters, concentration has the highest effect on the hydraulic performance of the slurry pump then particle size respectively. This numerical method causes to consider effective parameters of solid-liquid flow on the pump performance without any time-consuming experiments.

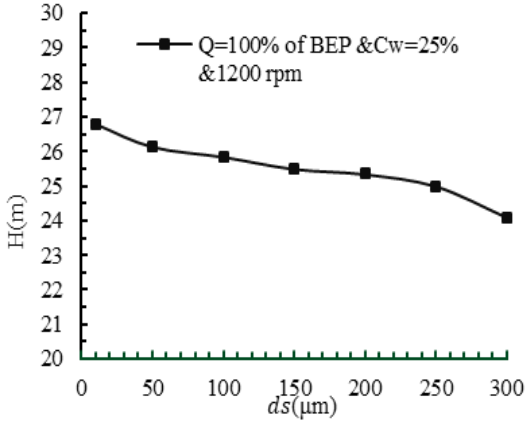

Fig. 8. The effect of diameter of solid particles on the slurry pump head.

4.2.4. Volumetric particle contour

Differences in solid phase dispersion were observed at various concentrations. With increasing volumetric concentration, more particles in the water separator are accumulated meanwhile in lower concentration, the solid phase contours are more uniform.

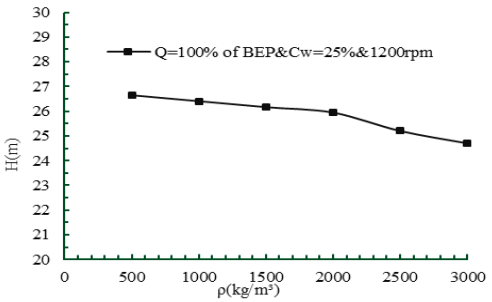

Fig. 9. The effect of density of solid particles on the slurry pump head.

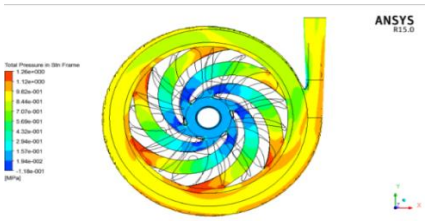

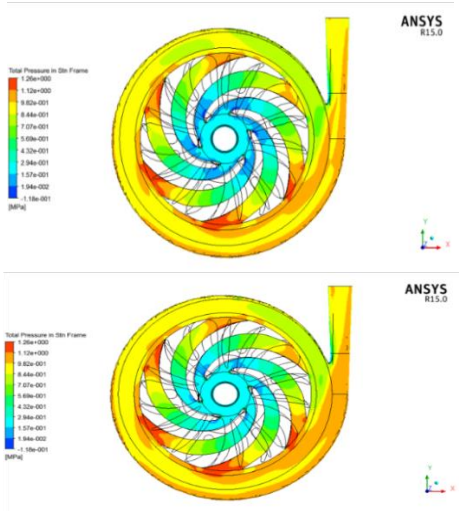

Fig. 10. Contour plots of pressure at a plane located in the middle height of the impeller-spiral volute interface for the best efficiency point rpm in concentration by weight; (a) 25 %, (b) 35%, and (c) 45%.

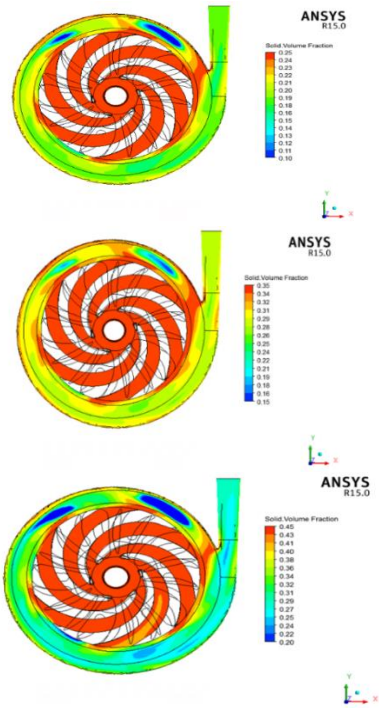

Fig. 11. Contour plot of volume fraction of solid particles at a plane located in the middle height of the impeller-spiral volute interface for the best efficiency point in concentration by weight; (a) 25 %, (b) 35%, and (c) 45%.

Table 4. Changes reduce the slurry pump head to water at different speeds.

Concentration	Head drop		
(%)	1200rpm	1400rpm	1600rpm
25	8.05	4.75	4.6

35	13.06	10.1	11.5
45	17.62	14.7	13

Table 5. Changes reduce the slurry pump efficiency to water at different speeds.

Concentration (%)	Head drop		
	1200rpm	1400rpm	1600rpm
25	9.3	5.3	4.8
35	11.7	8.75	6.7
45	18.7	16.5	15.1

Table 6. Changes reduce the pump head to water at different diameter and speeds in concentration by weight 25%.

Particle diameter	Head drop		
	1200rpm	1400rpm	1600rpm
50	3.15	1.4	1.1
100	4.25	1.9	1.15
200	6.1	3.5	2.8
250	8.05	4.75	4.6
300	10.75	7.15	7
350	12.8	9.6	9.5

Table 7. Changes reduce the pump head to water at different density and speeds in concentration by weight 25%.

Particle density	Head drop		
	1200rpm	1400rpm	1600rpm
500	1.35	1.15	0.9
1000	2.25	1.8	1.25
1500	3.15	3.3	2.5
2000	4.1	4.3	3.9
2500	6.7	4.45	4.1
3000	8.4	7.5	6.8

5. Conclusions

The main objective of this paper is the evaluation of the ability of computational fluid dynamics to simulate solid-liquid dual phase flow in the estimation of head and efficiency of a centrifugal slurry pump in different operating condition. In this paper, two-phase flow through an industrial centrifugal pump was simulated with the assumption of steady-state and utilizing the turbulent model and shear stress transmission based on Ulrine-Ulrine in the range of 45 to 120% of nominal discharge. After assuring the independence of numerical analysis from the computational network, the characteristic curves were compared with the simulation model, then the effect of changing the volume particle concentration on characteristic curves was gained and the correlation between numerical results and experimental data verified the numerical model. The effect of volumetric concentration at different discharges on performance curves was obtained and there is a good confirmation between the numerical result and experimental data. Among other variable parameters in the defined domain, the concentration was the most effective in the hydraulic performance of centrifugal slurry pump then particle diameter and particle density respectively, the effect of these parameters reduce with increasing rotational speed on the head drop. Repeating the numerical analysis process for different pumps and the effective parameters consideration of the slurry flow plays a crucial role in the proper prediction and enhancing the optimum performance of slurry flow or its re-design procedure.

References

[1] "S. Pump Handbook", Electronic Version, Warman company, Fifth Edition, pp. 1-56, (2009).

[2] B. Shi and J. Wei, "Numerical Simulation of 3D Solid-Liquid Turbulent Flow in a Low Specific Speed Centrifugal Pump: Performance Comparison of Four Geometric Models", *Adv. Mech. Eng.*, Vol. 6, pp. 1–8, (2014).

[3] B. K. Gandhi, S. N. Singh and V. Seshadri, "Effect of speed on the Performance Characteristics of a centrifugal slurry pump", *J. Fluid Eng.*, Vol. 128, No. 2, pp. 225-232, (2002).

[4] K. V. Pagalthivarthi, P. K. Gupta, V. Tyagi and M. R. Ravi, "CFD Predictions of Dense Slurry Flow in Centrifugal Pump Casings", *Int. J. Mech., Aerosp., Ind. Mechatronic Manuf. Eng.*, Vol. 5, No. 3, pp. 538-550, (2011).

[5] K. V. Pagalthivarthi, P. K. Gupta, V. Tyagi and M. R. Ravi, "CFD Prediction of Erosion Wear in Centrifugal Slurry Pumps for Dilute Slurry Flows", *J. Comput. Multiph. Flows*, Vol. 3, No. 4, pp. 225-245, (2011).

[6] M. Mehta, J. R. Kadambi, S. Sastry, J. M. Sankovic, M. P. Wernet, G. Addie and

R. Visintainer, "Particle Velocities in the Rotating Impeller of a Slurry Pump", *ASME/JSME Fluids Eng. Conf.*, San Diego, California, USA, July 30 – August 2, (2007).

[7] T. Wennberg, A. Sellgren and L. Whitlock, "Predicting the performance of centrifugal pumps handling complex slurries", *Int. Conf. Transp. Sedimentation Solid Part.*, June 23-25, (2008).

[8] A. Kumar, D. R. Kaushal and U. Kumar, Bend "Pressure Drop Experiments compared with Fluent", *Proc. Inst. Civ. Eng. Comput. Mech.*, Vol. 161, No. 1, pp. 35-42, (2008).

[9] S. Huang, X. Su and G. Qiu, "Transient numerical simulation for solid-liquid flow in a centrifugal pump by DEM-CFD coupling", *Eng. Appl. Comp. Fluid*, Vol. 9, No. 1, pp. 411-418, (2015).

[10] R. Tarodiya and B. K. Gandhi, "Numerical simulation of a centrifugal slurry pump handling solid-liquid mixture: Effect of solids on flow field and performance", *Adv. Powder Technol.*, Vol. 30, No. 10, pp. 2225-2239, (2019).

[11] S. Mohanty, O. Parkash and R. Arora, "Analytical and comparative investigations on counter flow heat exchanger using computational fluid dynamics", *J. Comput. Appl. Res. Mech. Eng.*, Vol. 10, No. 1, pp. 139-152, (2019).

[12] M. Blanco Alberto, F. O. J. Manuel and M. Andrés, "Numerical methodology for the CFD simulation of diaphragm volumetric pumps", *Int. J. Mech. Sci.*, Vol. 150, pp. 322-336, (2019).

[13] M. Alemi and R. Maia, "A comparative study between two numerical solutions of the Navier-Stokes equations", *J. Comput. Appl. Res. Mech. Eng.*, Vol. 6, No. 2, pp. 1-12, (2017).

[14] B. V. Ratish Kumar and K. B. Naidu, "A streamline up winding stream function-vorticity finite element analysis of Navier-Stokes equations", *Appl. Numer. Math.*, Vol. 13, No. 4, pp. 335-344, (1993).

[15] S. K. Lahiri, *Study on slurry flow modelling in pipeline*, PhD Thesis, Durgapur University, West Bengal, India. (2010).

[16] B. Shi and J. Wei, "Numerical Simulation of 3D Solid-Liquid Turbulent Flow in a Low Specific Speed Centrifugal Pump: Flow Field Analysis", *Adv. Mech. Eng.*, Vol. 6, pp. 1-11, (2015).

[17] F. R. Menter, "Two-Equation Eddy-Viscosity Turbulence Models for Engineering Applications", *AIAA J.*, Vol. 32, No. 8, pp. 1598–1605, (1994).

[18] Y. Gu, N. Liu, J. Mou, P. Zhou, H. Qian and D. Dai, "Study on solid–liquid two-phase flow characteristics of centrifugal pump impeller with non-smooth surface", *Adv. Mech. Eng.*, Vol. 11, No. 5, (2019).

[19] Z. Wang and Z. Qian, "Effects of concentration and size of silt particles on the performance of a double-suction centrifugal pump", *Energy*, Vol. 123, pp. 36-46, (2017).

[20] Y. Xiao, B. Guo, S. H. Ahn, Y. Lou, Z. Wang, G. Shi and Y. Li, "Slurry Flow and Erosion Prediction in a Centrifugal Pump after Long-Term Operation", *Energies*, Vol. 12, No.8, 1523, (2019).

[21] B. M. Bossio, A. J. Blanco and F. H. Hernández, "Eulerian-Eulerian Modeling of Non-Newtonian Slurries Flow in Horizontal Pipes", *ASME 2009 Fluids Eng. Div. Summer Meeting*, Vail, Colorado, USA, August 2–6, (2009).

[22] K. E. Burgess and S. A. Riezes, "The effect of sizing, specific gravity and concentration on the performance of centrifugal slurry pumps", *Proc. Inst. Mech. Eng.*, Vol. 190, No. 1, pp. 699-711, (1976).

[23] F. R. Menter, "Review of the shear-stress transport turbulence model experience from an industrial perspective", *Int. J. Comput. Fluid Dyn.*, Vol. 23, No. 4, pp. 305–316, (2009).

[24] *ANSYS CFX-Solver Theory Guide*, ANSYS CFX Release 15.0, (2013).

[25] B. Jafarzadeh, A. Hajari, M. M. Alishahi and M. H. Akbari, "The flow simulation of low specific speed high speed centrifugal pump", *Appl. Math. Model*, Vol. 35, No. 1, pp. 242-249, (2011).

[26] M. Aligoodarz, F. Ehsani Derakhshan and H. Karabi, "Numerical analysis of blade

roughness effects on gas turbine performance and flow field", *Modares Mech. Eng.*, Vol. 13, No. 13, pp. 112-120, (2014).

[27] T. Adams, C. Grant and H. Watson, "A Simple Algorithm to Relate Measured Surface Roughness to Equivalent Sand-grain Roughness", *Int. J. Mech. Eng. Mechatronics*, Vol. 1, No. 1, pp. 66–71, (2012).

[28] M. A. Dehghani, A. F. Najafi, S. A. Nourbakhsh and H. Shokoohmand, "Numerical investigation of fluid flow between the impeller and the casing on disk friction for centrifugal pump", *Modares Mech. Eng.*, Vol. 16, No. 4, pp. 163-174, (2016).

[29] M. Asuaje, F. bakir, S. Kouidri, F. Kenyery and R. Rey, "Numerical modelization of the flow in centrifugal pump: volute influence in velocity and pressure fields", *Int. J. Rotating Mach.*, Vol. 2005, No. 3, pp. 244–255, (2005).

[30] M. Shojaeefard, M. Tahani, M. Ehghaghi, M. Fallahian and M. Beglari, "Numerical study of the effects of some geometric characteristics of a centrifugal pump impeller that pumps a viscous fluid", *Comput. Fluids*, Vol. 60, pp. 61-70, (2012).

[31] J. F. Gülich, *Centrifugal Pumps*. 3rd Edition Springer, Verlag BerlinHeidelberg, (2014).

[32] M. Tan, S. Yuan, H. Liu, Y. Wang and K. Wang, "Numerical research on performance prediction for centrifugal pumps", *China J. Mech. Eng.*, Vol. 1, pp. 21-27, (2010).

[33] M. Ghaderi, A. F. Najafi and A. Nourbakhsh, "Estimation of a centrifugal pump slip factors at off-design condition using copmutational fluid dynamics", *Modares Mech. Eng.*, Vol. 15, No. 3, pp. 199-207, (2015).

How to cite this paper:

Mohammad Reza Aligoodarz, Mohsen Dalvandi and Abdollah Mehrpanahi, "Solid-phase effects on the performance of a centrifugal slurry pump using computational fluid dynamics,", *J. Comput. Appl. Res. Mech. Eng.*, Vol. 11, No. 1, pp. 243-255, (2021).

DOI: 10.22061/JCARME.2020.5977.1763

URL: https://jcarme.sru.ac.ir/?_action=showPDF&article=1230